Eur. Phys. J. A **16**, 599–601 (2003)
DOI 10.1140/epja/i2002-10128-3

**THE EUROPEAN PHYSICAL JOURNAL A**

# UCN production in superfluid helium

W. Schott[1,a], J.M. Pendlebury[2], I. Altarev[1,b], S. Gröger[1], E. Gutsmiedl[1], F.J. Hartmann[1], S. Paul[1], G. Petzoldt[1], P. Schmidt-Wellenburg[1], and U. Trinks[1]

[1] Physik-Department E18, TU- München, D-85747 Garching, Germany
[2] School of Chemistry, Physics and Environmental Science, University of Sussex, Brighton, Sussex, BNI 9QJ, UK

Received: 28 March 2002 / Revised version: 11 November 2002 /
Published online: 11 March 2003 – 
Communicated by T. Walcher

**Abstract.** Ultra-cold neutrons (UCN) are produced in superfluid helium by single- and multi-phonon excitation. The UCN production rate density $R_{\mathrm{II}}$ via multiphonons can be larger than that by one-phonon excitation $R_{\mathrm{I}}$ being due to the dependence of the incident neutron spectral flux density $\mathrm{d}\phi/\mathrm{d}\lambda$ on the wavelength $\lambda$.

**PACS.** 78.70.Nx Neutron inelastic scattering – 67.20.+k Quantum effects on the structure and dynamics of nondegenerate fluids (*e.g.*, normal phase liquid $^4$He) – 61.12.Ex Neutron scattering techniques (including small-angle scattering) – 29.25.Dz Neutron sources

The production of ultra-cold neutrons (UCN) via single-phonon excitation in superfluid helium has been proposed and discussed in great detail already in the 1970s by R. Golub, J.M. Pendlebury *et al.* [1,2]. It is based on the fact that superfluid helium has only a few possible states of motion —the famous phonon-roton dispersion curve— and exchange of energy and momentum between a free neutron with $T = (\hbar ck)^2/(2E_0)$ and a single phonon in the superfluid can take place only at the intersection point of the two dispersion curves, *i.e.*, only neutrons at a wavelength of about 9 Å can be transformed into the UCN energy range (mK). $T$, $\hbar k$ and $E_0 = 1.09 \cdot 10^{13}$ K are the neutron energy, momentum and rest energy, respectively.

Multiphonon excitation can increase the phase space for neutron downscattering and, thus, it is worth to study this process in more detail having in mind future superthermal UCN sources.

When cold and thermal neutrons pass through a volume of superfluid helium at very low temperature (ca. 0.4 K) [3], UCN of very high density (ca. $10^4\,\mathrm{cm}^{-3}$ compared with the density presently achieved at the ILL turbine of ca. $10^2\,\mathrm{cm}^{-3}$ [4]) can be produced by one- and multi-phonon processes, respectively. Since the $^4$He absorption cross-section is zero, the storage time is limited only by the neutron life time, the $^4$He purity and the storage volume wall absorption cross-section. High $^4$He purity and low absorption are obtained by filling the storage volume through a superleak (compressed $Al_2O_3$ powder with 200 Å grain size yielding a $10^{-10}$ impurity level [5]) and sputtering the walls with Be, respectively (high repulsive 252 neV Fermi potential at a small 7.6 mbarn absorption cross-section).

The macroscopic double differential cross-section for neutron downscattering in superfluid helium from the energy $T...T+\mathrm{d}T$ to the UCN energy $T'...T'+\mathrm{d}T'$ is given by [6]

$$\mathrm{d}^2\Sigma/(\mathrm{d}\Omega\,\mathrm{d}T') = n_{^4\mathrm{He}}\sigma_{\mathrm{b}}\,k's(q,\hbar\omega)/(4\pi\,k),$$

where $n_{^4\mathrm{He}} = 2.185 \cdot 10^{22}\,\mathrm{cm}^{-3}$ is the $^4$He atom density, $\sigma_{\mathrm{b}} = 1.34 \cdot 10^{-24}$ cm$^2$ the bound nuclear cross-section, $k$ and $k'$ the initial and final neutron wave vectors and $s = s_{\mathrm{I}} + s_{\mathrm{II}}$ the scattering functions due to single-phonon and multiphonon excitation, respectively, depending on the momentum transfer $q = |\vec{k} - \vec{k'}|$ and energy transfer $\hbar\omega = T - T'$. $s_{\mathrm{II}}(q,\hbar\omega)$ of 0.5 K superfluid helium has been measured recently for $0.6 \le q \le 2.2\,\mathrm{\AA}^{-1}$ [7]. However, the covered region in $q$ and $\hbar\omega$ is too small to be used for calculating the UCN production for all $T$ values of the incident neutrons.

Since $q$ is in the range

$$k - k' \le q \le k + k', \tag{1}$$

and the $k'/k$ ratio is $k'/k \le 1.8 \cdot 10^{-2}$, $\mathrm{d}\Omega$ is given by $\mathrm{d}\Omega = 2\pi\,\mathrm{d}q/k'$ [8] yielding

$$\mathrm{d}\Sigma/\mathrm{d}T' = n_{^4\mathrm{He}}\sigma_{\mathrm{b}}\,/(2k)\int_{k-k'}^{k+k'} s(q,\hbar\omega)\mathrm{d}q\,. \tag{2}$$

[a] e-mail: wschott@e18.physik.tu-muenchen.de
[b] On leave of absence from PNPI, Gatchina, Russia

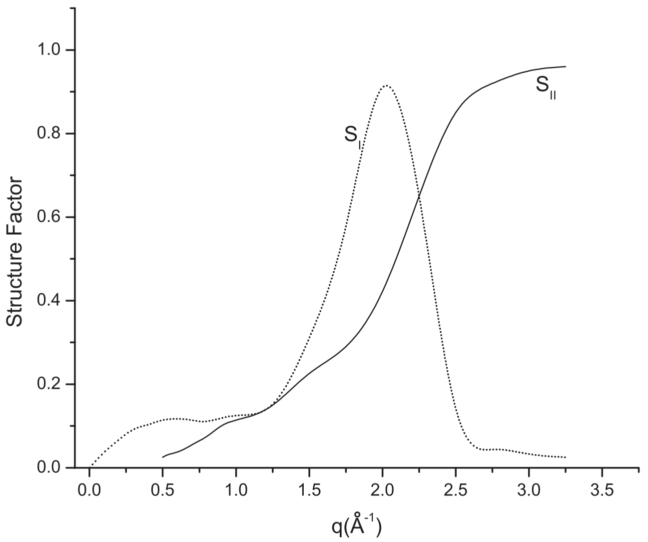


**Fig. 1.** Structure factor in superfluid helium due to one- ($S_{\rm I}$) and multi-phonon ($S_{\rm II}$) excitation *vs.* momentum transfer $q$ [9].

The double differential UCN production rate density $\mathrm{d}^2R = \mathrm{d}^2(R_{\rm I} + R_{\rm II}), R_{\rm I}$ and $R_{\rm II}$ being the single- and multi-phonon contributions, results to be

$$\mathrm{d}^2R = \mathrm{d}\phi \cdot \mathrm{d}\Sigma, \tag{3}$$

where $\mathrm{d}\phi$ is the differential incoming neutron flux density.

When UCN are produced, the momentum and energy transfer are to a good approximation equal to the initial neutron momentum $k$ and energy $T$, respectively, both described by the incident neutron wavelength $\lambda$. $s_{\rm I}(\lambda)$ consists just of a sharp peak at $\lambda = \lambda^* = 8.99\,\text{Å}$, the crossing point of the free neutron and the acoustical phonon dispersion curves, with $s_{\rm I}(\lambda^*) = 0.15\,\mathrm{K}^{-1}, \delta\lambda = (\mathrm{d}\lambda/\mathrm{d}q)\delta q = 0.27\,\text{Å}$ width (fig. 2a below) and $\delta q = 2k_{\rm c}$ (cf. eq. (1)), $k_{\rm c}$ being the UCN momentum corresponding to $T_{\rm c}$, where $T_{\rm c} = 2.73\,\mathrm{mK}$ is the critical UCN energy inside the Be coated storage volume filled with helium. $s_{\rm I}(\lambda^*)$ results from the one-phonon structure factor at $q^*, S_{\rm I}(q^*) = 0.105$ [9] (fig. 1), where $S_{\rm I}(q^*)$ can be written as $S_{\rm I}(q^*) = s_{\rm I}(\lambda^*)(\mathrm{d}T/\mathrm{d}\lambda)_{\lambda^*}\delta\lambda$. $q^* = 0.7\,\text{Å}^{-1}$ is the neutron momentum transfer at $\lambda^*$.

Inserting $\mathrm{d}\Sigma$ (eq. (2)) into eq. (3) $\mathrm{d}^2R_{\rm I}$ can be integrated over $T$ because of the $\delta$-function type $s_{\rm I}(\lambda)$ (cf. coherent one-phonon inelastic-scattering cross-section [10]). The following integration over $T'$ yields [8],

$$R_{\rm I} = (\mathrm{d}\phi/\mathrm{d}\lambda)_{\lambda^*}(\lambda^*/3)\alpha\, n_{^4\mathrm{He}}\sigma_{\rm b}S_{\rm I}(q^*)(T_{\rm c}/T^*)^{3/2}\,,$$

where $(\mathrm{d}\phi/\mathrm{d}\lambda)_{\lambda^*}$ is the incident neutron spectral flux density, $T^* = 11.85$ K the neutron energy and $\alpha = 1.45$ a numerical factor due to the dispersion curve slopes, all at $\lambda^*$, respectively.

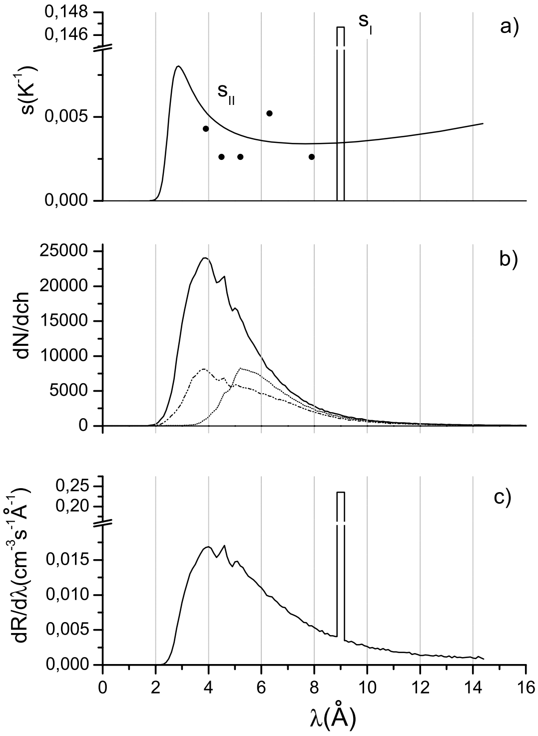


**Fig. 2.** a) One-phonon ($s_{\rm I}$) and multiphonon ($s_{\rm II}$) scattering functions *vs.* incident neutron wavelength $\lambda$. The full dots denote measured $s_{\rm II}$ values [7]. b) Count rate of the neutron spectral flux density measurement at the HMI cold-n guide end *vs.* $\lambda$ [12]. The dotted lines denote measurements with the counter displaced in the horizontal plane by $\pm 1$ cm from the maximum flux density. c) Resulting spectral UCN production rate density *vs.* $\lambda$.

The multiphonon structure factor $S_{\rm II}(q)$ (fig. 1) is given by

$$S_{\rm II} = \int_0^\infty s_{\rm II}(q,\hbar\omega)\mathrm{d}\hbar\omega = (1/N_0)\int_0^\infty(\partial n(q,\hbar\omega)/\partial\hbar\omega)\mathrm{d}\hbar\omega, \tag{4}$$

where $n(q,\hbar\omega)$ is the number of multiphonon states at $q$ and $\hbar\omega$. $N_0$ is the total number of multiphonon states, $s_{\rm II}$ being

$$s_{\rm II}(q,\hbar\omega) = (1/N_0)(\partial n(q,\hbar\omega)/\partial\hbar\omega). \tag{5}$$

$S_{\rm II}(q)$ can also be written as

$$S_{\rm II}(q) = (1/N_0)\int_0^q(\mathrm{d}N(q')/\mathrm{d}q')\mathrm{d}q'\,,$$

being normalized to 1 for large $q$ [9], where $N(q') = \int_0^\infty(\partial n(q',\hbar\omega)/\partial\hbar\omega)\mathrm{d}\hbar\omega$ means the number of multiphonon states at $q'$.

$\mathrm{d}S_{\rm II}(q)/\mathrm{d}q = (1/N_0)(\mathrm{d}N/\mathrm{d}q)$ is the relative differential number of multiphonon states along the $q$-axis, which is

**Table 1.** Measured multiphonon scattering function $(s_{\rm II})_G(\lambda)$ along the free neutron dispersion curve by M.R. Gibbs *et al.* [7].

| $q\,(\text{Å}^{-1})$ | $\hbar\omega\,(\text{meV})$ | $\lambda\,(\text{Å})$ | $(s_{\rm II})_G$ $\cdot 10^{-2}\,(\text{meV}^{-1})$ |
|---|---|---|---|
| 0.8 | 1.33 | 7.85 | 3 |
| 1.0 | 2.07 | 6.28 | 6 |
| 1.2 | 2.98 | 5.24 | 3 |
| 1.4 | 4.06 | 4.49 | 3 |
| 1.6 | 5.30 | 3.93 | 5 |

projected onto the $\hbar\omega$-axis using the free neutron dispersion relation by $(\mathrm{d}S_{\rm II}/\mathrm{d}q)(\mathrm{d}q/\mathrm{d}\hbar\omega)$ yielding a good approximation for $s_{\rm II}(\lambda)$ along the free neutron dispersion curve, if $s_{\rm II}(q,\hbar\omega)$ is a rather flat, unstructured distribution *vs.* $\hbar\omega$, as it is the case for the multiphonon excitations of superfluid helium [7].

$$(\mathrm{d}S_{\rm II}/\mathrm{d}q)(\mathrm{d}q/\mathrm{d}\hbar\omega) \quad \text{can be written as (eq. (4))}$$
$$(\mathrm{d}S_{\rm II}/\mathrm{d}q)(\mathrm{d}q/\mathrm{d}\hbar\omega) = (1/N_0)(\partial/\partial\hbar\omega)\int_0^\infty (\partial n/\partial q')\mathrm{d}q',$$

which yields $s_{\rm II}(q,\hbar\omega)$ (eq. (5)), if $\partial n/\partial q'$ is integrated only up to $q$ instead of to $\infty$.

Thus, the above approximation gives a somewhat too large $s_{\rm II}$ at small $q$ or large $\lambda$ and the correct $s_{\rm II}$ at large $q$ or small $\lambda$.

*I.e.*, $s_{\rm II}$ is approximately given by

$$s_{\rm II} \approx (\mathrm{d}S_{\rm II}(q)/\mathrm{d}q)(\mathrm{d}q/\mathrm{d}T) = (\mathrm{d}S_{\rm II}(q)/\mathrm{d}q)q^{-1}\,2.08\cdot 10^{-2}\,\mathrm{K}^{-1} \qquad (6)$$

with $q$ in $\text{Å}^{-1}$.

$s_{\rm II}(\lambda)$ is slowly varying and covers a wide $\lambda$ range (fig. 2a). For comparison, measured multiphonon scattering function values $(s_{\rm II})_G(\lambda)$ [7] are given in table 1 and fig. 2a, showing a reasonable agreement with $s_{\rm II}(\lambda)$ obtained from eq. (6), even for the measured points with the largest $\lambda$.

$\mathrm{d}^2R_{\rm II}$ can, therefore, be integrated over $T'$ (cf. eq. (3) and (2)) yielding [8]

$$\mathrm{d}R_{\rm II}/\mathrm{d}\lambda = n_{^4\mathrm{He}}\sigma_{\rm b}\sqrt{2E_0}T_{\rm c}^{3/2}/(3\pi\hbar c)\mathrm{d}\phi/\mathrm{d}\lambda\,\lambda\,s_{\rm II}\,.$$

The differential production rate densities $\mathrm{d}R_{\rm I}/\mathrm{d}\lambda$ and $\mathrm{d}R_{\rm II}/\mathrm{d}\lambda$ depend on the differential flux $\mathrm{d}\phi/\mathrm{d}\lambda$, which is calibrated absolutely using the thermal equivalent flux $\Phi$ [11] by

$$\mathrm{d}\phi/\mathrm{d}\lambda = \Phi\lambda_0(\mathrm{d}N/\mathrm{d}ch)/\int_0^\infty \lambda(\mathrm{d}N/\mathrm{d}ch)\mathrm{d}\lambda\,,$$

yielding with, *e.g.*, $\Phi = 2\cdot 10^8\,\mathrm{cm}^{-2}\mathrm{s}^{-1}$ at the HMI cold-neutron beam guide [12], $\lambda_0 = 1.8\,\text{Å}$ and $\mathrm{d}N/\mathrm{d}ch$, the measured counts per time channel, when a time-of-flight method is used (fig. 2b), $\mathrm{d}\phi/\mathrm{d}\lambda = 959.4\,\mathrm{d}N/\mathrm{d}ch\,\mathrm{cm}^{-2}\mathrm{s}^{-1}\text{Å}^{-1}$.

The resulting $\mathrm{d}R/\mathrm{d}\lambda = \mathrm{d}(R_{\rm I}+R_{\rm II})/\mathrm{d}\lambda$ *vs.* $\lambda$ is shown in fig. 2c. The integrals are $R_{\rm I} = 6.4\cdot 10^{-2}\,\mathrm{cm}^{-3}\mathrm{s}^{-1}$ and $R_{\rm II} = 7.5\cdot 10^{-2}\,\mathrm{cm}^{-3}\mathrm{s}^{-1}$, respectively. For a nearly thermal $\mathrm{d}\phi/\mathrm{d}\lambda$ with a maximum matching with that of $s_{\rm II}$, $R_{\rm II}$ exceeds $R_{\rm I}$ correspondingly more. *E.g.*, the $\mathrm{d}\phi/\mathrm{d}\lambda$ at the end of the FRM QRII cold-neutron guide connected with a 1 l liquid $H_2$ cold source, has its maximum at about 3 Å coinciding with that of $s_{\rm II}$ yielding a $R_{\rm II}/R_{\rm I}$ ratio of $R_{\rm II}/R_{\rm I} = 1.6$.

## References


1. R. Golub, J.M. Pendlebury, Phys. Lett. A **82**, 337 (1977).
2. R. Golub, D.J. Richardson, S.K. Lamoreaux, *Ultra-cold Neutrons* (Adam Hilger, 1991) and references therein.
3. H. Yoshiki *et al.*, Cryogenics **34**, 277 (1994).
4. A. Steyerl *et al.*, Phys. Lett. A **116**, 347 (1986).
5. H. Yoshiki, private communication, 2002.
6. W. Marshall, S.W. Lovesey, *Theory of Thermal Neutron Scattering* (Oxford at the Clarendon Press, Oxford, 1971).
7. M.R. Gibbs *et al.*, J. Low Temp. Phys. **120**, 55 (2000).
8. J.M. Pendlebury, internal note, 1982.
9. R.A. Cowley, D.B. Woods, Can. J. Phys. **49**, 177 (1971).
10. V.F. Turchin, *Slow Neutrons* (Israel Program for Scientific Translations, Jerusalem, 1965), translated from *Medlennye Neitrony* (Gosatomizdat, Moskva, 1963).
11. B. Doerschel, V. Schuricht, J. Steuer, *Praktische Strahlenschutzphysik* (Spektrum Akademischer Verlag, Heidelberg, 1992).
12. E. Korobkina, private communication, 2001.